Received: 22 October 2019 | Revised: 18 February 2020 | Accepted: 27 February 2020

DOI: 10.1111/ejss.12951

ORIGINAL ARTICLE

European Journal of Soil Science WILEY

A century of liming affects the Mg isotopic composition of the soil and crops in a long-term agricultural field at Berlin-Dahlem, Germany

Yi Wang[1,2] | **Bei Wu**[1] | **Anne E. Berns**[1] | **Roland Bol**[1] | **Frank Wombacher**[3] | **Frank Ellmer**[4] | **Wulf Amelung**[1,5]

[1]Institute of Bio- and Geosciences: Agrosphere (IBG-3), Forschungszentrum Jülich GmbH, Jülich, Germany

[2]Institute for Environmental Research, Biology 5, RWTH Aachen University, Aachen, Germany

[3]Institute of Geology and Mineralogy, Universität zu Köln, Köln, Germany

[4]Department of Crop and Animal Sciences, Humboldt-Universität zu Berlin, Berlin, Germany

[5]Institute of Crop Science and Resource Conservation (INRES), Soil Science and Soil Ecology, Universität Bonn, Bonn, Germany

Correspondence
Yi Wang, Institute of Bio- and Geosciences: Agrosphere(IBG-3), Forschungszentrum Jülich GmbH, Wilhelm-Johnen-Straße, 52425 Jülich, Germany.
Email: yi.wang@fz-juelich.de

Funding information
Bundesministerium für Bildung und Forschung, Grant/Award Number: 031B0026C 2015; China Scholarship Council, Grant/Award Number: 201506320204

Abstract

Liming is widely used to alleviate soil acidity in western and central Europe, but its role in the cycling of magnesium (Mg) in arable soil–plant systems is still ambiguous. Here, we systematically analysed Mg concentrations and the natural Mg stable isotope compositions (δ^{26}Mg) of two Mg pools in soil profiles and a major crop (winter rye) in a long-term German agricultural experimental field that has been managed with and without liming since 1923. The results showed that the δ^{26}Mg signatures of the bulk soil Mg pool in the studied Albic Luvisol displayed limited variation with depth and between the liming treatments. In contrast, the exchangeable soil Mg pool exhibited an increase in δ^{26}Mg values with depth down to 50 cm, which was more pronounced in the limed plots. We attributed this enrichment of light Mg isotopes in upper layers to the Mg addition from "Dolokorn 90" lime, as well as to the removal of heavy Mg isotopes by plant uptake. The subsequent use of a simple isotope-mixing model suggested that only 25% of the remaining Mg in the soil exchangeable pool stemmed from the last liming practice. The other parts of the exchangeable soil Mg pool had either interacted with the bulk soil matrix or had been utilized by the plants. Almost 100 years of liming enhanced Mg uptake by the vegetation, probably via elevated Mg contents in the grain, and reflected by the stronger depletion of heavy Mg isotopes in the soil exchangeable Mg pool relative to non-limed plots. Whole winter rye plants were enriched in heavy Mg isotopes but they displayed similar Mg isotope compositions among plant organs in all plots, indicating identical Mg uptake and translocation strategies in the different trials. Tracing the stable isotope compositions of soil and plant

Mg thus opens novel opportunities to evaluate soil management impacts on the cycling and fate of this essential nutrient in agricultural systems.

Highlights

- Mg concentrations and stocks in an Albic Luvisol were more heterogeneous in subsoils than in topsoils
- The variation of Mg isotope compositions of bulk soil was limited with depth and between liming treatments
- Liming induced a pronounced negative shift of δ^{26}Mg values in soil exchangeable Mg pools down to a 50-cm soil depth
- Uptake of Mg by plants in limed plots was enhanced relative to that in non-limed plots

KEYWORDS

Albic Luvisol, exchangeable Mg, liming, Mg isotopes, soil–plant system, winter rye

1 | INTRODUCTION

Magnesium (Mg) is an essential macronutrient for plant growth, functioning in a series of enzymes and related physiological and biochemical processes, such as photosynthesis (Maguire & Cowan, 2002; Pasternak, Kocot, & Horecka, 2010). Insufficient supply of Mg to plants impairs root growth and reduces plants' tolerance of environmental stress (e.g., Bose, Babourina, & Rengel, 2011; Cakmak & Kirkby, 2008), thus lowering yield and quality of crops in arable farming systems (Gerendas & Führs, 2013). However, when nutrients in topsoil are deficient and/or plant roots elongate into deep layers, subsoil can provide nutrients for plant growth (Kautz et al., 2013). In a pioneering study using pot experiments, Mg supply from the subsoil was shown to have great potential for alleviating Mg deficiency of spring wheat (Kuhlmann & Baumgartel, 1991). However, there are still few data available and little consensus on the use of nutrients from subsoils under different soil management conditions on the field scale. One difficulty in elucidating subsoil Mg uptake is the lack of a reliable analytical approach, which is capable of distinguishing nutrients taken up from the subsoil from those available in the surface horizons.

As Mg isotopes are fractionated by a number of biotic and abiotic processes, recent studies on Mg isotope geochemistry have shown the great potential of utilizing Mg isotope systematics as a tool to trace the biogeochemical cycle of Mg in the terrestrial environment (see reviews, Schmitt et al., 2012; Teng, 2017). Riverine waters have been shown to be generally depleted in heavy Mg isotopes relative to the rocks in their silicate catchments (e.g., Brenot, Cloquet, Vigier, Carignan, & France-Lanord, 2008; Liu, Teng, Rudnick, McDonough, & Cummings, 2014; Mavromatis, Prokushkin, Pokrovsky, Viers, & Korets, 2014; Tipper et al., 2006). This was ascribed to water–rock interactions that preferentially released isotopically light Mg during dissolution processes, which was confirmed in experimental studies (Ryu et al., 2016; Wimpenny et al., 2010). A larger extent of Mg isotope fractionation has been detected during the formation of secondary minerals following silicate weathering processes: the δ^{26}Mg values in secondary minerals were up to +1.5‰ higher than in their parent bedrocks, which was attributed to the preferential incorporation of heavy Mg isotopes into newly formed clay minerals (e.g., Huang, Teng, Wei, Ma, & Bao, 2012; Liu et al., 2014; Teng, Li, Rudnick, & Gardner, 2010; Tipper, Lemarchand, Hindshaw, Reynolds, & Bourdon, 2012). However, several studies also reported an enrichment of light Mg isotopes in bulk soils relative to their parent minerals (Li, Beard, Li, & Johnson, 2014; Opfergelt et al., 2012, 2014; Pogge von Strandmann et al., 2008). Processes such as ion exchange, successive adsorption–desorption of Mg on clay minerals and clay mineral transformation, apart from Mg incorporation, have been assumed to be the reason for such contrary isotope signatures (Huang et al., 2012; Ma et al., 2015; Wimpenny, Colla, Yin, Rustad, & Casey, 2014; Wimpenny, Yin, Tollstrup, Xie, & Sun, 2014). In addition, external Mg inputs (e.g., aeolian factors or rain) may also significantly contribute to the δ^{26}Mg isotope signatures in the environment (Liu et al., 2014). For example, depositions due to sea spray dominated the exchangeable Mg pool in the surface horizon of Icelandic soils (Opfergelt et al., 2014). On the other hand, biological processes can also induce Mg isotope fractionation. Most studies to date showed that plants, either cultivated under laboratory conditions or in the field, preferentially take up heavy Mg isotopes, although this fractionation could be species specific and affected by associated mycorrhizal fungi (e.g., Black,

Epstein, Rains, Yin, & Casey, 2008; Bolou-Bi, Poszwa, Leyval, & Vigier, 2010; Bolou-Bi, Vigier, Poszwa, Boudot, & Dambrine, 2012; Kimmig, Holmden, & Belanger, 2018; Mavromatis et al., 2014; Tipper et al., 2012; Uhlig, Schuessler, Bouchez, Dixon, & von Blanckenburg, 2017).

The overall natural variation of Mg isotopes has ranged as much as +7‰ in the Earth's surface environment (Teng, 2017). However, limited information is available on the variation of δ^{26}Mg isotope signatures in arable soils. The only study on agricultural soil so far by Gao et al. (2018) reported increasing values of bulk soil δ^{26}Mg with soil depth, from −0.85‰ in topsoil to −0.59‰ in soil at 100-cm depth, in a paddy soil developed from a latosol because of the decreasing Mg content retained on exchangeable sites. Similarly, soil management practices such as liming can also lead to differing δ^{26}Mg values, particularly if the applied lime contains Mg of a different isotope composition from that found in the bulk soil, such as dolomite (Bolou-Bi et al., 2016). We hypothesize that differing isotope compositions of Mg in topsoil and subsoil can be used to evaluate the effect of soil managements on Mg uptake by crops. In this study, we systematically analysed the Mg concentrations and natural isotope compositions along soil profiles and crop (winter rye) samples in field plots subjected to a controlled liming practice for nearly 100 years of the long-term agricultural experimental station at Berlin-Dahlem, Germany (Krzysch et al., 1992). The analyses allowed us to examine the effect of long-term agricultural liming practice on: (a) the Mg isotope compositions in different soil Mg pools and (b) the Mg uptake by crops using Mg isotopes as a proxy. We suspected that the overall results would improve our understanding of the acquisition of Mg from the entire soil profile and could thus provide a potential new approach to evaluate the effect of soil managements on the fate and uptake efficiency of essential nutrients in agricultural ecosystems.

2 | MATERIALS AND METHODS

2.1 | Study site, sampling and sample preparation

The studied long-term experimental field is located in Berlin-Dahlem, Germany (52°28′02″ N, 13°17′49″ E). Different agricultural managements have been practised since the year 1923 to investigate the effects of phosphorus fertilization, liming and tillage depth on crop growth and yields (Köhn & Ellmer, 2009). Vegetation practices in this field trial are performed as an annual rotation, with cereals and non-cereal crops planted alternately each year since 1967. The climate is semi-continental with a mean annual temperature of 9.9°C and an average annual precipitation of 562 mm. According to the FAO (IUSS Working Group WRB, 2014), the soil at this experimental site is classified as an Albic Luvisol, developed from glacial till. The soil texture is sandy to loamy sand, dominated by sand particles that comprise 65–75% of soil weight in the topsoil (0–30 cm) and 40–60% in the subsoil (30–100 cm) (Hobley & Prater, 2019). The field site is heterogeneous with regard to textural changes with soil depth from 40 to >100 cm (Figure S1, Sümer, 2012).

In the present work, plots with and without liming were investigated and each treatment included three field replicates. All of these plots received phosphorus fertilizer (20 kg ha^{-1} a^{-1}) and farmyard manure (15 t ha^{-1} a^{-1}), and all plots were ploughed to 28-cm depth before crop sowing. The lime application was performed regularly in intervals of 2 to 4 years since 1923. As the lime sources varied during the course of the experiment, no exact balance of calcium (Ca) and Mg additions could be reconstructed. In 2014, the lime product Dolokorn 90 (containing 30% $MgCO_3$) was applied with 920 kg ha^{-1} to the limed plots, in which 79.3 kg ha^{-1} Mg was added equivalently.

Field sampling was carried out in the year 2016 before renewed liming. Two soil cores, down to 100 cm, were collected at random places in each plot. The soil coring technique followed that of the German inventory of agriculture and was tested and described previously for this purpose (Bauke et al., 2018; Walter, Don, Tiemeyer, & Freibauer, 2016). Each soil core was then separated into six layers (with depth 0–15 cm for Ap1, 15–30 cm for Ap2, 30–40 cm for Bw1, 40–50 cm for Bw2, 50–70 cm for Ael/Bt and 70–100 cm for the Bt horizon). The depth segments were carefully chosen based on soil profile description and test cores taken adjacent to the main experiment site. Soil segments of the same depth from these two soil cores were pooled on site.

All pooled soil samples were lyophilized, ground in an agate mortar to break down the soil aggregates and passed through a 2-mm sieve before chemical and physical analyses. Determination of dry bulk density and pH of the soil samples were obtained with the method reported by Bauke et al. (2018). Generally, soil pH ($CaCl_2$) in the limed plots was one unit higher than that in the non-limed plots (Table S3).

Whole plants of winter rye (*Secale cereale*) grown in these plots were taken out when they were at the flowering stage in May 2017. Roots and shoots were separated on site and stored in a dry-ice box immediately in the field. In the laboratory, the shoots were divided into stems, leaves and spikes and, together with the roots, were thoroughly rinsed with Milli-Q water to remove fine soil particles and dusts. The root samples were

additionally ultrasonicated at room temperature for 10 min to remove adsorbed soil particles. The cleaned plant samples were then immediately frozen at −20°C and freeze-dried. The dried plant organs were milled to a powder using a custom-made ball mill equipped with metal-free plastic bottles and tungsten carbide milling balls (Collomix Viba 330, Collomix GmbH, Gaimersheim, Germany). The remaining soil and plant samples were stored for further analysis.

2.2 | Extraction of Mg from soil and plant samples

Total digestion of soil samples was performed using lithium meta/tetraborate fusion at 1050°C for 3 hr. The concentrations of Mg (termed as $Mg_{total\ soil}$) and other nutrient elements were determined by inductively coupled plasma optical emission spectroscopy (ICP-OES, iCap, Thermo Fisher Scientific, Dreieich, Germany) at Forschungszentrum Jülich GmbH.

For the purpose of Mg isotope analyses, a pressurized microwave-assisted acid digestion system (turboWAVE inert, MILESTONE Srl, Sorisole, Italy) was used to digest soil and plant samples, as well as the lime product Dolokorn 90, in the present work because lithium meta/tetraborate fusion introduced a large amount of matrix. The microwave-assisted extraction removed between 70 and 100% (average 88%) Mg from the soil matrix. Precisely weighed samples were suspended in 2.5 ml distilled concentrated HNO_3 (68%) and 1.5 ml H_2O_2 (30%) in perfluoroalkoxy alkanes (PFA) vessels. The vessels were then pressurized to approx. 35 to 40 bars in a closed cylinder and subsequently heated step-wise to 225°C. The obtained Mg from soil was regarded as bulk soil Mg ($Mg_{bulk\ soil}$) in this work (Figure S2). An in-house soil standard (Luvisol, collected in Klein-Altendorf, Germany (50°37′9″ N, 6°59′29″ E)), validated against the certified NIST 2709a San Joaquin Soil standard, was used to validate each run with respect to Mg concentration. The SRM NIST1575a Pine Needles standard was used to validate the analytical procedure for plant samples (Table S1). An acid blank per run was used to check for contamination.

The exchangeable pool of Mg in soil is usually defined as the Mg pool that is available for plant uptake (Metson, 1974). For extraction of the exchangeable Mg pool in soil (Mg_{exch}), the NH_4-acetate extraction method reported by Bolou-Bi et al. (2012) and Gao et al. (2018) was applied. Thirty millilitres of 1 M NH_4-acetate (pH = 7) solution was added to 3 g soil and the mixture was shaken at a speed of 220 oscillations per minute for 2 hr. The sample suspension was then centrifuged at 6,000 *g* for 15 min. The supernatant was collected and filtered through a 0.45-μm polytetrafluorethylene filter. The filtrate was then transferred into a Savillex® PFA vial and dried down. Ultrapure HNO_3 and H_2O_2 were used to remove organic matter through a process of repeated dry-down and re-dissolution. The residue was finally dissolved into 1 M HNO_3 solution for Mg purification. The Mg content in the sample before and after drying and re-dissolving the filtrate was analysed at Forschungszentrum Jülich GmbH by inductively coupled plasma mass spectrometry (ICP-MS, Agilent 7,900, Agilent, Germany) to evaluate potential Mg losses. The uncertainty of ICP-MS measurements was less than 5%. The concentration of Mg in the acid blank was below the detection limit of the ICP-MS (< 50 ng/L), which is negligible compared to the samples.

2.3 | Magnesium purification and isotope analysis

Separation of Mg from matrix elements was carried out by cation exchange chromatography using Bio-Rad AG50W-X8 resin (200–400 mesh, Bio-Rad, Hercules, California, USA), following the modified procedure outlined in Table S2 (Teng, Wadhwa, & Helz, 2007; Wombacher, Eisenhauer, Heuser, & Weyer, 2009). The purified Mg eluents after column chemistry were then dried down in Savillex PFA vials at 90°C and re-dissolved in 2 ml 1 M distilled HNO_3. The recoveries of Mg and the absence of matrix elements were examined by measuring elemental concentrations on ICP-MS. Solutions with yield recovery of Mg over 95% as well as absence of matrix elements (matrix/Mg ratio < 5%) were submitted for isotope measurement.

Magnesium isotope ratios were determined at Forschungszentrum Jülich GmbH by multi-collector ICP-MS (MC-ICP-MS, Nu Plasma ||, Nu Instruments Ltd, Wrexham, UK) by introducing sample solutions into the source region through a twister quartz spray chamber with a helix (Glass Expansion, West Melbourne, Australia) equipped with a glass nebulizer (MicroMist, Glass Expansion) at an uptake rate of ca. 100 μL min^{-1}. The standard-sample-standard bracketing method was applied to correct the instrumental mass bias using SRM NIST 980 as the bracketing Mg reference material. Each sample was measured at least three times. The Mg isotope composition is initially expressed as δ notation relative to this standard in permil unit:

$$\delta^{x}Mg^{sample}_{NIST980} = \left[\frac{\left({}^{x}Mg/{}^{24}Mg\right)_{sample}}{\left({}^{x}Mg/{}^{24}Mg\right)_{NIST980}} - 1\right] \times 1000$$

where x represents the mass 25 or 26. The long-term reproducibility of the MC-ICP-MS analyses was 0.07‰

for $\delta^{25}Mg$ and 0.09‰ for $\delta^{26}Mg$ (2SD, $n > 50$), respectively. The three-isotope plot was used to assess possible interferences that would induce mass-independent fractionation. The analysed isotope ratios displayed mass-dependent fractionation only, following the exponential law (Figure S3). The analyses were validated by repeated and in-laboratory cross-checked measurements of the in-house soil standard and the SRM NIST 1575a Pine Needles standard for soil and plant samples, respectively (Table S1).

Due to the reported heterogeneity of SRM NIST 980, the $\delta^{26}Mg$ values relative to the purchased SRM NIST 980 used for bracketing ($\delta^{26}Mg^{sample}_{NIST980}$) were then normalized relative to the proposed zero-delta reference material DSM3 (Dead Sea Magnesium, Galy et al., 2003) as $\delta^{26}Mg^{sample}_{DSM3}$ with the following equation (Young & Galy, 2004):

$$\delta^{26}Mg^{sample}_{DSM3} = \delta^{26}Mg^{sample}_{NIST980} + \delta^{26}Mg^{NIST980}_{DSM3} + 0.001 \cdot \delta^{26}Mg^{sample}_{NIST980} \cdot \delta^{26}Mg^{NIST980}_{DSM3}$$

where $\delta^{26}Mg^{SRM\,980}_{DSM3}$ (-3.91 ± 0.09‰, 2SD, $n = 12$) is the isotope composition of our SRM NIST 980 relative to the DSM3, which was determined at the Institute of Geology and Mineralogy at the University of Cologne, Germany. The $\delta^{26}Mg$ values given in the present study are reported relative to DSM3 without the subscript.

2.4 | Data calculation

The Mg isotope composition of the shoot ($\delta^{26}Mg_{shoot}$) and/or of the bulk plant ($\delta^{26}Mg_{plant}$) was calculated using the following mass balance equation:

$$\delta^{26}Mg_{shoot\ or\ plant}(‰) = \sum\left(\delta^{26}Mg_i \times \frac{m_i c_i}{\sum m_i c_i}\right)$$

where m_i (in grams), C_i (in μg g^{-1}) and $\delta^{26}Mg_i$ (‰) were the dry biomass, Mg concentration and isotope composition of the plant organ i (root, stem, leaf and spike/seed).

The apparent difference in Mg isotope composition between different Mg pools was calculated using:

$$\Delta^{26}Mg_{A-B} = \delta^{26}Mg_A - \delta^{26}Mg_B$$

The statistical analyses were carried out by OriginPro 2015 (Version b9.2.272). Here, we used a paired-sample *t*-test to evaluate the significant difference ($p < .05$), within each soil block, among six soil layers, among plant organs, and between the exchangeable Mg pools in soil and plants. The effect of liming practice on Mg concentration and isotope composition of both soil and plant samples was tested with a two-sample *t*-test between limed and non-limed fields, following an F-test used for the equal variance checking ($p < .05$).

An isotope-mixing model based on mass balance calculation was developed to track the sources of Mg that are described in section 4.1. A detailed description of the isotope-mixing model can be found in the Supporting Information.

3 | RESULTS

3.1 | Magnesium concentrations, stocks and isotope compositions in bulk soil

The Mg concentration in the total Mg pool of soil increased from the surface soil to the deeper soil layers in both treatments with and without liming practice, varying from 866 to 3,915 mg kg^{-1} (Figure 1a, Table S3). In the topsoil (0–30 cm), Mg concentrations in these two treatments were found to be similar with small variability between plots (Figure 1a). By contrast, Mg concentration in the subsoil below the ploughing depth of 28 cm showed larger spatial variations, as expected for the heterogeneous processes of soil movement in the last ice age (Chmielewski & Köhn, 1999). Multiplying Mg concentrations by bulk density yielded the Mg stock in each soil layer, illustrated here in a cumulative form as Mg accumulation in bulk soil from the surface down to this layer (Figure 1b). The soils of the two treatments exhibited a similar range of Mg stocks and isotope compositions within the first 100 cm of soil depth (Figure 1b,c). The Mg isotope compositions in the studied Albic Luvisol did not change significantly, either along the soil depth or between the treatments, with average $\delta^{26}Mg_{bulk\ soil}$ values of $+0.08 \pm 0.02$‰ and $+0.09 \pm 0.02$‰ (SE, $n = 18$) for the limed and non-limed plots, respectively (Figure 1c, Table S3).

3.2 | Magnesium concentrations in the soil exchangeable Mg pool and in winter rye

Similar to the total Mg pool in soil, the exchangeable Mg pool displayed a general increase in Mg concentration with soil depth and exhibited homogeneity among plots in the upper horizons of the soil profile compared with the soil layers below 30 cm depth (Figure 2). The Mg concentrations of winter rye plants grown in both limed and non-limed plots varied within a much narrower range and did not display a significant difference between the

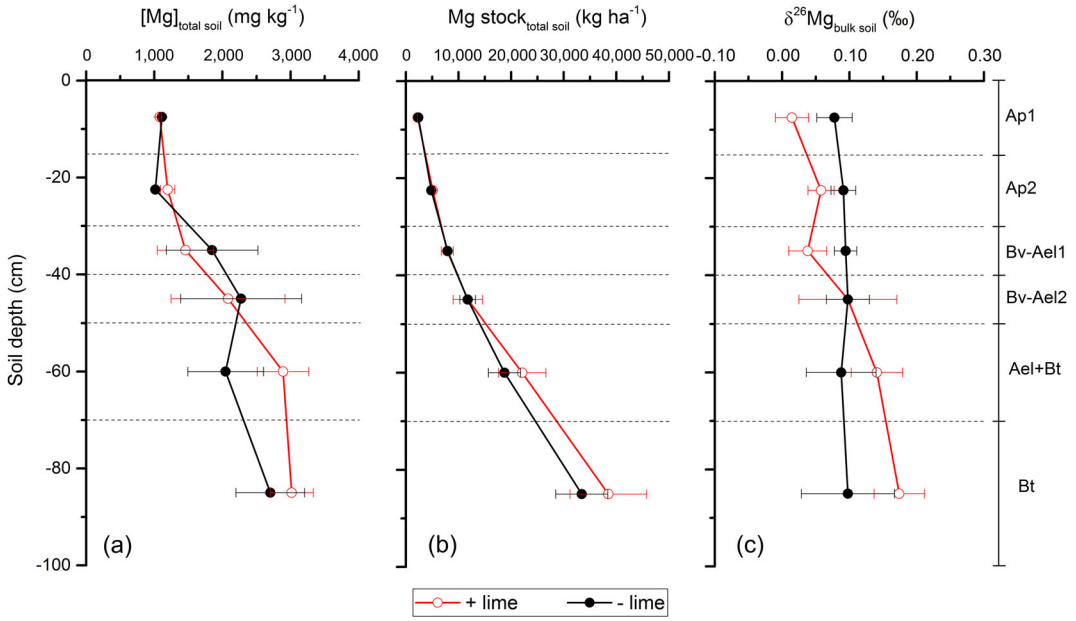

FIGURE 1 Depth profiles of total Mg concentrations (a), total Mg stocks (b) and bulk soil Mg isotope compositions (c) in soil samples collected from experimental fields with (open red) or without (solid black) liming management. Horizon designations given according to German classification of a representative key soil profile at the experimental site, where Ap is the ploughed topsoil, Bv-Ael and Ael correspond to an eluvial horizon, and Ael + Bt and Bt to an argic horizon according to the World Reference Base (IUSS Working Group WRB, 2015). Data are shown as mean ± SE of three field replicates. Larger error bars in (a) indicate heterogeneity of Mg concentration in the upper subsoil [Color figure can be viewed at wileyonlinelibrary.com]

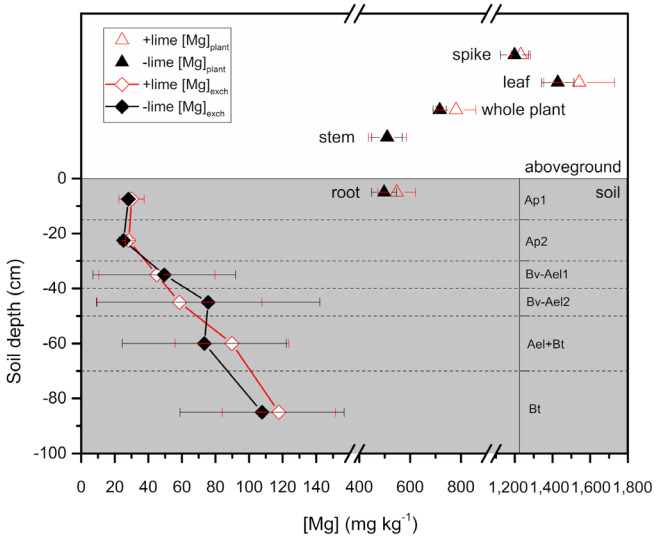

FIGURE 2 Concentration of exchangeable Mg in soil ($(Mg)_{exch}$) along the soil depth (diamond) and in each plant organ of winter rye (triangle) in limed (open red) and non-limed (solid black) plots. Horizon designations and descriptions are shown in Figure 1. Data are given as mean value ± SE of three field replicates [Color figure can be viewed at wileyonlinelibrary.com]

treatments (780 ± 78 vs. 716 ± 26 mg kg^{-1} for the limed and non-limed plots, respectively, SE, $n = 3$; Figure 2). Among plant organs, leaves and spikes contained about two to three times larger Mg concentrations than roots and stems (Figure 2, Table S4).

3.3 | Magnesium isotope compositions in the soil exchangeable Mg pool and in winter rye

Compared with the bulk soil, the exchangeable Mg pool of the soil was enriched in light Mg isotopes. The Mg isotope signatures of the exchangeable pool went down to −1.54‰ in the surface layer in the limed plots (Figure 3). Unlike the limited Mg isotopic variations in bulk soil Mg, the Mg in the exchangeable pool became isotopically heavier with increasing soil depth. At 0–50-cm depth, liming led to a shift to more negative $\delta^{26}Mg$ values than in the non-limed plots, with a difference in $\delta^{26}Mg$ values between the two treatments ($\Delta^{26}Mg_{limed\text{-}non} = \delta^{26}Mg_{limed} - \delta^{26}Mg_{non}$) of up to −0.20‰.

The whole plants of winter rye in both treatments were isotopically heavier than the exchangeable Mg pool in the soil layer of 0–15-cm depth, where most of the roots had prevailed, with those grown in the limed plots generally displaying more negative $\delta^{26}Mg$ values than those in the non-limed plots (Figure 3). As for the Mg isotope compositions of plant organs, the stems and leaves were enriched in light Mg isotopes compared with the

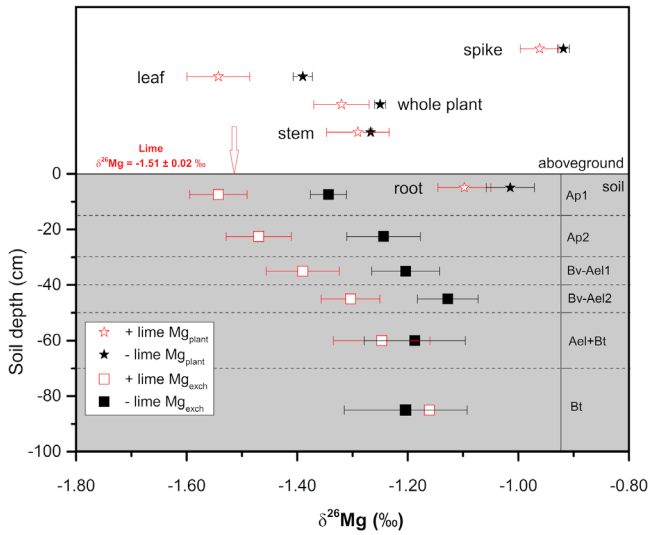

FIGURE 3 Isotope compositions of the exchangeable Mg pool in soil (square) along the soil depth and in each plant organ (star) in limed (open red) and non-limed (solid black) plots. The red arrow represents the addition of lime in limed plots with a δ^{26}Mg of −1.51 ± 0.02 ‰ (2SD, $n = 3$). For horizon designations and descriptions see caption for Figure 1. Data are presented as mean value ± SE of three field replicates [Color figure can be viewed at wileyonlinelibrary.com]

roots, whereas the spikes exhibited the heaviest Mg isotope composition among all plant organs studied (Figure 3). This sequence of δ^{26}Mg values was observed for plants growing both in the limed and non-limed plots.

4 | DISCUSSION

4.1 | Total Mg and exchangeable Mg pools in the studied Albic Luvisol

Magnesium isotope signatures in soil systems are determined not only by an individual process but rather by a series of processes during material deposition and pedogenesis, resulting in the range of natural soil δ^{26}Mg values from −1.0 to +1.8‰ (Gao et al., 2018). The present study displayed for the first time the Mg isotope compositions of an Albic Luvisol with a limited range of δ^{26}Mg values from +0.01 to +0.17‰. The bulk soil of this Albic Luvisol also did not show any pronounced alteration of δ^{26}Mg values with depth (less than +0.16‰), despite the fact that total and exchangeable Mg concentrations increased along with soil depths in both limed and non-limed fields (Figures 1 and 2). This confirms that the Mg isotope compositions in the investigated plots were not controlled by the Mg content. As the studied Albic Luvisol is characterized by lessivage (i.e., downward migration of clay particles), the lack of Mg isotope fractionation implies that the formation of illuvial and alluvial horizons did not alter the δ^{26}Mg distribution in the soil profile. This also gives support to the hypothesis that the lessivage process during soil formation transported clay particles that were intact (Blume et al., 2016), thus avoiding isotope fractionation at our site. The Mg isotope compositions of the bulk soil in the studied field therefore mainly reflected the values of their parent material.

Liming has been applied to our field site every 2 to 4 years since 1923. In the year 2014, the lime product applied was changed from mainly $CaCO_3$ (>90%) to Dolokorn 90, which contained 30% $MgCO_3$. This means that additional Mg (79.3 kg Mg ha^{-1}) from the lime was added to the soil, given that the applied amount of lime product in that year was 920 kg ha^{-1}. As $MgCO_3$ is water soluble, it can be considered to be readily plant available. This Mg supply is larger than that which could have been removed by rye harvests (≤ 15 kg Mg $year^{-1}$; Landwirtschaftskammer NRW, 2017), even if some additional Mg might have been allocated by roots and non-cereal crops such as the maize grown in the year before. Nevertheless, the soil exchangeable Mg pool hardly differed in concentration between limed and non-limed plots (Figure 2), despite the fact that the amount of the additional Mg through liming was equivalent to 24% of the Mg_{exch} stock in the soil layers down to 50 cm depth of the limed plots (Figure S4). Yet, the additions of Mg with liming were small (< 4%) relative to the total Mg stock in the soils. Also, the contributions of exchangeable Mg to the bulk Mg pool ($Mg_{exch}/Mg_{bulk\ soil}$) in the 0–50-cm soil-depth interval were significantly larger in the limed plots than in the non-limed ones, with small variations among plots (Figure S4). Therefore, we expected that the size of the soil exchangeable Mg pool depended mostly on interactions with the parent soil rather than on recent liming practice, with heterogeneity possibly smoothing differences between sites in regard to the patterns of soil Mg_{exch} concentrations.

The exchangeable Mg pool was, on average, isotopically significantly lighter than that of the bulk Mg pool in soil, both in the plots with and without liming practices (Figures 1 and 3). This finding is in good agreement with earlier studies and can be partially ascribed to mineral weathering (Gao et al., 2018; Opfergelt et al., 2014). An Albic Luvisol is typically dominated by vermiculite and illite (also kaolinite in some cases) that show a 2:1 layer structure (Brigatti, Galan, & Theng, 2006; Mile & Mitkova, 2012). Such three-layered clay minerals have a high capacity to store isotopically light Mg ions in their interlayers and thus to release them when needed. As a result, these clay minerals tend to promote the prevalence of isotopically light Mg isotopes in the

exchangeable soil Mg pool. It should also be noted that, however, as all treatments occurred in direct vicinity, soil mineralogy should not have affected the differences between limed and non-limed plots. Nevertheless, for a given site it can thus be expected that the Mg isotope composition of the exchangeable Mg pool in soil depends on the amounts of Mg absorbed into these clay minerals as the exchangeable form (Gao et al., 2018; Ma et al., 2015; Mile & Mitkova, 2012). However, in the present work, the Mg isotope composition of the exchangeable pool showed independence from the soil clay contents (Figure S5; Table S3). The depletion of heavy Mg isotopes in the upper part of the soil profile (0–50-cm depth), specifically in the limed plots (Figure 3), indicated that apart from mineral weathering combined with subsequent adsorption onto clay minerals, further processes determined the isotope composition of exchangeable Mg. One process was certainly the lime addition, whereas another would most likely be plant uptake. As the dolomite lime was enriched in light Mg isotopes ($-1.51 \pm 0.02‰$, SE, $n = 3$, Figure 3), which is in line with the general observation that carbonate minerals are enriched in light Mg isotopes (Galy, Bar-Matthews, Halicz, & O'Nions, 2002; Li, Chakraborty, Beard, Romanek, & Johnson, 2012; Wang, Teng, Rudnick, & Li, 2015), addition of lime products with isotopically light Mg indeed resulted in lighter Mg isotope compositions in the exchangeable Mg pool of the soil down to 50 cm.

We attempted to trace the contributions from lime products using Mg isotope analyses. However, except for the Dolokorn 90 applied in 2014, the lime applied before 2014 containing over 90% $CaCO_3$ may also contain small amounts of Mg. As the previous lime products are not available, analyses of the Mg contents and isotope compositions are therefore not feasible for those lime products. We thus assumed that the Mg in the previously applied $CaCO_3$ products was limited. In addition, it is worth noting that the $\delta^{26}Mg_{exch}$ values in the soil layers below 50-cm depth were identical within error, in the limed and non-limed plots (Figure 3), indicating that the effect of liming on Mg isotope composition did not reach deeper soil layers at the time of sampling. We thus assumed that all the added lime was retained in the top 50 cm of soil.

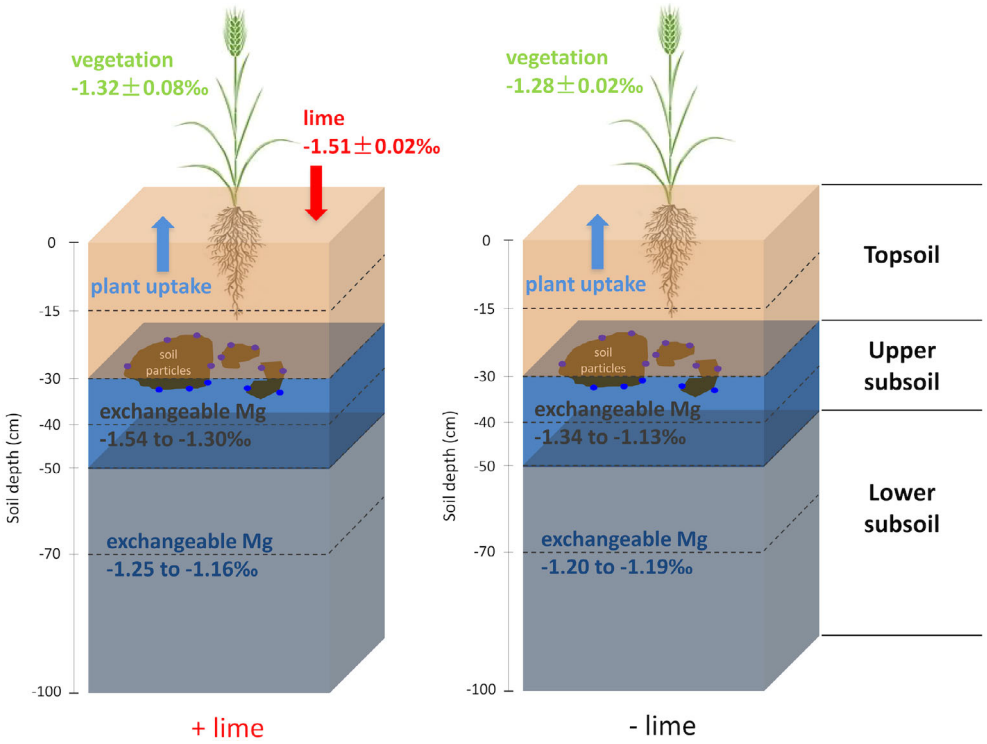

FIGURE 4 Conceptual diagram of the isotope-mixing model to calculate the Mg isotope mass balance between the plant and exchangeable Mg pool in the present agricultural system with (left) and without (right) liming practice. Soil profiles were divided into three horizons, topsoil, upper subsoil and lower subsoil, with soil depth of 0–30, 30–50 and 50–100 cm, respectively (blocks marked in different colours). We considered the topsoil (brown) and upper subsoil (blue) as main compartments according to the hypothesis presented in section 4.2. The Mg isotope compositions in the exchangeable Mg pools are given as a range of the δ^{26}Mg values for the upper half of the profile (topsoil (brown) + upper subsoil (blue)) and the lower half (lower subsoil (grey)), respectively (Table S3). The δ^{26}Mg values of the crop (green) are given as calculated mean of the whole plant ± SE of three field replicates (Table S4) [Color figure can be viewed at wileyonlinelibrary.com]

To clarify the respective contributions of the lime addition and the plant uptake to the negative shift of $\delta^{26}Mg_{exch}$ in limed plots, we developed an isotope-mixing model for mass balance calculation using the Dolokorn Mg isotope composition as input variable (Figure 4, see Supporting Information for detailed description of the isotope-mixing model). The average Mg $stock_{exch}$ in the top 50 cm of soil was consistent between these two field trials (334 ± 193 kg ha^{-1} for limed and 332 ± 187 kg ha^{-1} for non-limed plots, SE, $n = 3$; Table S3) and the calculated average $\delta^{26}Mg_{exch}$ values of the soil compartments (0–50 cm) were -1.41 ± 0.07‰ and -1.21 ± 0.18‰ in limed and non-limed plots, respectively (SE, $n = 3$). Although these two values overlapped within error, the offset between the exchangeable Mg pool in both plots was much the same ($\Delta^{26}Mg = +0.20 \pm 0.09$, SE, $n = 4$) at all depths above 50 cm (Figure 3). Using the non-limed plots as reference, the calculated value of $\delta^{26}Mg_{exch}$ in the limed plots due to the most recent lime addition would be -1.26 ± 0.16‰ based on the mass balance calculation. The actual shift of $\delta^{26}Mg_{exch}$ by 0.05‰ induced by the lime addition only accounted for 25% of the difference in $\delta^{26}Mg_{exch}$ values between limed and non-limed plots ($\Delta^{26}Mg_{limed\text{-}non} = -0.20$‰, section 3.2), which means that the negative shift of $\delta^{26}Mg_{exch}$ in limed plots did not only result from the lime addition. Instead, other processes such as plant uptake and recycling through plant biomass, as well as interactions with the bulk soil as indicated above, controlled the current pool size of Mg in the exchangeable pool. Besides, the removal of heavy Mg isotopes by crops can be considered as a main reason for the offset in the Mg_{exch} isotope composition between treatments; that is, the Mg fraction removed by plant uptake in limed plots was slightly larger than that in non-limed plots, as also reflected by Mg concentration measurements in the plants, even if in the presently sampled winter rye plants in limed plots these differences were not significant (Table S4). Parts of the difference could well also be attributed to the removal of heavy Mg isotopes by maize, which was grown in the field before the winter rye. The field documentation showed that the maize plants took up about 5 kg ha^{-1} more Mg in limed plots than in non-limed plots. As plants are generally reported to preferentially take up heavy Mg isotopes (Bolou-Bi et al., 2012; Gao et al., 2018), decades of removal of more heavy Mg isotopes compared with non-limed plots thus has additionally contributed to the isotopically lighter Mg composition of Mg_{exch} in limed plots compared with non-limed plots. Long-term liming practice is, to a certain extent, expected to enhance the uptake of Mg by the agricultural field crops in the studied field. Hence, our study showed that using stable isotope tracing allowed us to estimate the respective contribution from lime addition and plant uptake to the $\delta^{26}Mg$ value of the exchangeable soil Mg pool with an isotope-mixing model.

The preferential uptake of heavy Mg isotopes may be species specific, as Kimmig et al. (2018) recently reported absence of uptake-induced Mg isotope fractionation in field-grown sugar maple. However, such a tree is very different from crops. Graminaceous plants, to date, are reported to enrich heavy Mg isotopes such as wheat (Black et al., 2008), clover and rye-grass (Bolou-Bi et al., 2010), grass (Opfergelt et al., 2014) and rice (Gao et al., 2018). We thus expected that other crops grown on the studied field for rotation (e.g., maize) had the same enrichment of heavy Mg isotopes as winter rye. Additionally, recent studies have also shown that microbes (e.g., mycorrhizal fungi) whose activities can be influenced by culture substrate and pH, can also fractionate Mg isotopes linked with microbial uptake of Mg (Fahad, Bolou-Bi, Kohler, Finlay, & Mahmood, 2016; Pokharel et al., 2017, 2018). Kimmig et al. (2018) reported an absence of uptake-related Mg isotope fractionation by field-grown sugar maple and attributed such lack of fractionation to the colonization of arbuscular mycorrhizae on roots. In the present study, alleviation of soil acidity by liming may facilitate microbial activities, which can also enhance the Mg uptake by crops due to the symbiotic relationships between winter rye plants and arbuscular mycorrhizae (Yadav, Akhtar, & Panwar, 2015). However, analyses of soil microbes in the studied field were not included in the present work. Further studies could focus on the microbe-root surface for better understanding the plant-induced Mg isotope fractionations at the field scale.

4.2 | Magnesium isotope fractionation in winter rye

In cropped fields, any released Mg in soil solutions can be taken up by the vegetation, subjecting it to biotic-induced Mg isotope fractionations. Previous studies showed that plants preferentially take up heavier Mg isotopes and thus exhibited more positive $\delta^{26}Mg$ values than the Mg source (Black et al., 2008; Bolou-Bi et al., 2010, 2012; Uhlig et al., 2017). The range of so-far reported apparent uptake-induced differences in $\delta^{26}Mg$ ($\Delta^{26}Mg_{plant\text{-}source}$) has been estimated to be −0.10 to +1.21‰ at both the laboratory and field scales, with average value of 0.14‰ (Kimmig et al., 2018; Pokharel et al., 2018). At our site, the $\delta^{26}Mg$ values of whole plants were -1.32 ± 0.06‰ and -1.25 ± 0.01‰ for the limed and non-limed plots, respectively (SE, $n = 3$). These values were lower than previously reported for field-grown rice (−0.92‰, Gao et al., 2018), grass (−0.28‰, Opfergelt

et al., 2014) and spruce (−0.32‰, Bolou-Bi et al., 2012), which was attributed to the plant species and reservoir effects of Mg sources (Gao et al., 2018). However, the apparent difference in isotope composition between the whole rye plants and the Mg_{exch} pool in the surface soil (0–15-cm depth) ($\Delta^{26}Mg_{plant\text{-}source}$) was +0.18 ± 0.04‰ (SE, $n = 6$; Table S4), in agreement with the reported $\Delta^{26}Mg_{plant\text{-}source}$ ranges with regards to field studies specifically (−0.10 to +0.64‰ in field studies only), and was close to the yielded average value (+0.14‰, Kimmig et al., 2018).

The positive apparent difference in Mg isotope compositions between root and aboveground organs ($\Delta^{26}Mg_{root\text{-}shoot}$ + 0.20 to +0.31‰) indicates Mg fractionation during the root–shoot translocation with an enrichment of light Mg isotopes in shoots, particularly in leaves (Figure 3). Previous studies indicated similar results by suggesting that free Mg cations are translocated upwards in the xylem sap due to higher diffusion rates for the light Mg isotopes (Bolou-Bi et al., 2010, 2012). Isotopically light Mg is then accumulated in leaf cells for plant physiological activities (e.g., photosynthesis), leading to a negative shift of $\delta^{26}Mg$ values in the leaves. Additionally, the transport of Mg from leaf to spike in the phloem contributes to the depletion of heavy Mg isotopes in leaves, as Mg is associated with organic compounds (e.g. polyphosphate) in leaves and transported by the phloem sap from leaf to storage organs, a process that preferentially transports heavy Mg isotopes (Bolou-Bi et al., 2010).

It is noteworthy that the liming practice did not change Mg internal translocation processes within the plants, as both the whole winter rye and plant organs displayed similar $\delta^{26}Mg$ values between treatments (Figure 3). The extent of isotope fractionation either by root–shoot translocation ($\Delta^{26}Mg_{root\text{-}shoot}$ = +0.24 ± 0.03‰ in limed plots vs. +0.27 ± 0.03‰ in non-limed plots, SE, $n = 3$) or by leaf–spike translocation ($\Delta^{26}Mg_{leaf\text{-}spike}$ = −0.58 ± 0.10‰ in limed plots vs. -0.47 ± 0.01‰ in non-limed plots, SE, $n = 3$) was similar in the investigated winter rye grown in the limed and non-limed plots. A main reason for this observation is likely to be that the crops under consideration did not suffer from adverse environmental growth stress, such as Mg-deficient soil conditions and heavy soil acidification in the non-limed plots (Figure 2). Winter rye plants grown in limed and non-limed plots thus adapted identical Mg uptake and translocation strategies that resulted in the same extent of Mg isotope fractionation.

5 | CONCLUSION

In the present study, Mg isotope compositions were systematically analysed in arable soil profiles and in winter rye crops in the plots with and without liming treatments. Long-term liming practices did not induce significant Mg isotope fractionation in the total Mg pool of the studied Albic Luvisols. However, the $\delta^{26}Mg$ values of the soil exchangeable Mg pool in limed plots decreased relative to those in non-limed plots at the depth of 0–50 cm. This was attributed to (i) the input of light Mg isotopes by lime product addition and (ii) increased removal of heavy Mg isotopes by plant uptake, which accounted for 25% and 75%, respectively, as illustrated by the isotope-mixing model. We conclude that tracing the stable isotope compositions of nutrients such as Mg in soil–plant systems can support agricultural managements in making nutrient use more effective. By using the isotope-mixing model here, we were able to identify the contribution from either lime addition or plant uptake to the isotope composition of the exchangeable soil Mg pool. Similarly, other isotope models can also be established to investigate, for example, nutrient uptake depth and uptake efficiency under different agricultural managements. Hence, tracing nutrient isotopes in arable systems provides a novel opportunity to evaluate the effect of soil management on the nutrient flows in agricultural systems.

ACKNOWLEDGEMENTS

The authors would like to thank Dr Kathlin Schweitzer and Michael Baumecker for compiling and providing the historical data and their help in field sampling. Our work was funded by the German Federal Ministry of Education and Research (BMBF) in the project of "Soil as a Sustainable Resource for the Bioeconomy – BonaRes", project "BonaRes (Module A): Sustainable Subsoil Management - Soil^3; subproject 3" (grant number 031B0026C, 2015). Y. Wang also appreciates the China Scholarship Council (CSC) for financial support (scholarship number 201506320204). We are grateful to the two anonymous reviewers for their constructive comments and suggestions.

CONFLICT OF INTEREST

The authors state that this work has no conflict of interest.

AUTHOR CONTRIBUTIONS

Y. Wang developed the original idea, processed sample treatment, analysed data, wrote the manuscript and is the guarantor. B. Wu, A.E. Berns, R. Bol and W. Amelung contributed to the development of the laboratory work and manuscript. F. Wombacher helped with the method validation and manuscript. F. Ellmer helped with the field running and sampling.

DATA AVAILABILITY STATEMENT

The data of the present study will be available at BonaRes Data Portal: https://datenzentrum.bonares.de/research-data.php

ORCID

Yi Wang https://orcid.org/0000-0001-5413-4248
Bei Wu https://orcid.org/0000-0003-1784-1992

REFERENCES

Bauke, S., von Sperber, C., Tamburini, F., Gocke, M., Honermeier, B., Schweitzer, K., … Amelung, W. (2018). Subsoil phosphorus is affected by fertilization regime in long-term agricultural experimental trials. *European Journal of Soil Science*, *69*, 103–112.

Black, J. R., Epstein, E., Rains, W. D., Yin, Q. Z., & Casey, W. H. (2008). Magnesium-isotope fractionation during plant growth. *Environmental Science & Technology*, *42*, 7831–7836.

Blume, H.-P., Brümmer, G. W., Horn, R., Kandeler, E., Kögel-Knabner, I., Kretzschmar, R., … Wilke, B.-M. (2016). *Scheffer/Schachtschabel: Lehrbuch der Bodenkunde*. Heidelberg, Germany: Springer-Verlag.

Bolou-Bi, E. B., Dambrine, E., Angeli, N., Pollier, B., Nys, C., Guerold, F., & Legout, A. (2016). Magnesium isotope variations to trace liming input to terrestrial ecosystems: A case study in the Vosges mountains. *Journal of Environmental Quality*, *45*, 276–284.

Bolou-Bi, E. B., Poszwa, A., Leyval, C., & Vigier, N. (2010). Experimental determination of magnesium isotope fractionation during higher plant growth. *Geochimica et Cosmochimica Acta*, *74*, 2523–2537.

Bolou-Bi, E. B., Vigier, N., Poszwa, A., Boudot, J. P., & Dambrine, E. (2012). Effects of biogeochemical processes on magnesium isotope variations in a forested catchment in the Vosges Mountains (France). *Geochimica et Cosmochimica Acta*, *87*, 341–355.

Bose, J., Babourina, O., & Rengel, Z. (2011). Role of magnesium in alleviation of aluminium toxicity in plants. *Journal of Experimental Botany*, *62*, 2251–2264.

Brenot, A., Cloquet, C., Vigier, N., Carignan, J., & France-Lanord, C. (2008). Magnesium isotope systematics of the lithologically varied Moselle river basin, France. *Geochimica et Cosmochimica Acta*, *72*, 5070–5089.

Brigatti, M., Galan, E., & Theng, B. (2006). Structures and mineralogy of clay minerals. *Developments in Clay Science*, *1*, 19–86.

Cakmak, I., & Kirkby, E. A. (2008). Role of magnesium in carbon partitioning and alleviating photooxidative damage. *Physiologia Plantarum*, *133*(4), 692–704.

Chmielewski, F. M., & Köhn, W. (1999). The long-term agrometeorological field experiment at Berlin-Dahlem, Germany. *Agricultural and Forest Meteorology*, *96*, 39–48.

Fahad, Z. A., Bolou-Bi, E. B., Kohler, S. J., Finlay, R. D., & Mahmood, S. (2016). Fractionation and assimilation of Mg isotopes by fungi is species dependent. *Environmental Microbiology Reports*, *8*, 956–965.

Galy, A., Bar-Matthews, M., Halicz, L., & O'Nions, R. K. (2002). Mg isotopic composition of carbonate: Insight from speleothem formation. *Earth and Planetary Science Letters*, *201*, 105–115.

Galy, A., Yoffe, O., Janney, P. E., Williams, R. W., Cloquet, C., Alard, O., … Carignan, J. (2003). Magnesium isotope heterogeneity of the isotopic standard SRM980 and new reference materials for magnesium-isotope-ratio measurements. *Journal of Analytical Atomic Spectrometry*, *18*, 1352–1356.

Gao, T., Ke, S., Wang, S. J., Li, F. B., Liu, C. S., Lei, J., … Wu, F. (2018). Contrasting Mg isotopic compositions between Fe-Mn nodules and surrounding soils: Accumulation of light Mg isotopes by Mg-depleted clay minerals and Fe oxides. *Geochimica et Cosmochimica Acta*, *237*, 205–222.

Gerendas, J., & Führs, H. (2013). The significance of magnesium for crop quality. *Plant and Soil*, *368*, 101–128.

Hobley, E. U., & Prater, I. (2019). Estimating soil texture from vis–NIR spectra. *European Journal of Soil Science*, *70*, 83–95.

Huang, K. J., Teng, F. Z., Wei, G. J., Ma, J. L., & Bao, Z. Y. (2012). Adsorption- and desorption-controlled magnesium isotope fractionation during extreme weathering of basalt in Hainan Island, China. *Earth and Planetary Science Letters*, *359*, 73–83.

IUSS Working Group WRB. (2014). *World Reference Base for Soil Resources International soil classification system for naming soils and creating legends for soil maps. World Soil Resources Reports, No. 106* (). Rome, Italy: FAO.

Kautz, T., Amelung, W., Ewert, F., Gaiser, T., Horn, R., Jahn, R., … Köpke, U. (2013). Nutrient acquisition from arable subsoils in temperate climates: A review. *Soil Biology & Biochemistry*, *57*, 1003–1022.

Kimmig, S. R., Holmden, C., & Belanger, N. (2018). Biogeochemical cycling of Mg and its isotopes in a sugar maple forest in Quebec. *Geochimica et Cosmochimica Acta*, *230*, 60–82.

Köhn, W., & Ellmer, F. (2009). *Dauerfeldversuche in Brandenburg und Berlin. Beiträge für eine nachhaltige Landwirtschaftliche Bodennutzung (Long-term field tests in Brandenburg and Berlin. Contributions to sustainable agricultural land use)* (Vol. 10, p. 216). Frankfurt (Oder), Germany: State Office for Consumer Protection, Agriculture and Land Consolidation, Department of Agriculture and Horticulture, Series in Agriculture.

Krzysch, G., Gaesar, K., Becker, K., Brodowski, M., Dressler, U.-B., Grimm, J., Jancke, G., Krause, S. & Schlenther, L. (1992). Einfluß von langjährig differenzierten Bewirtschaftungsmaßnahmen und Umweltbelastungen auf Bodenfruchtbarkeit und Ertragsleistung eines lehmigen Sandbodens (Influence of long-term differentiated management measures and environmental pollution on soil fertility and yield of a loamy sandy soil). Final Report of the Interdisciplinary Research Project, IFP 15/2, at the Institute of Crop Research, Technische Universität Berlin, Margraf, Berlin, Germany. ISSN 0177–6673.

Kuhlmann, H., & Baumgartel, G. (1991). Potential importance of the subsoil for the P and Mg nutrition of wheat. *Plant and Soil*, *137*, 259–266.

Landwirtschaftskammer Nordrhein-Westfalen (2017): Ratgeber Pflanzenbau und Pflanzenschutz, 22. Aufl. – Bonn, Germany: Landwirtschaftskammer Nordrhein-Westfalen Pressestelle.

Li, W. Q., Beard, B. L., Li, C. X., & Johnson, C. M. (2014). Magnesium isotope fractionation between brucite (Mg(OH)(2)) and Mg aqueous species: Implications for silicate weathering and biogeochemical processes. *Earth and Planetary Science Letters*, *394*, 82–93.

Li, W. Q., Chakraborty, S., Beard, B. L., Romanek, C. S., & Johnson, C. M. (2012). Magnesium isotope fractionation during precipitation of inorganic calcite under laboratory conditions. *Earth and Planetary Science Letters*, *333*, 304–316.

Liu, X. M., Teng, F. Z., Rudnick, R. L., McDonough, W. F., & Cummings, M. L. (2014). Massive magnesium depletion and isotope fractionation in weathered basalts. *Geochimica et Cosmochimica Acta*, *135*, 336–349.

Ma, L., Teng, F. Z., Jin, L., Ke, S., Yang, W., Gu, H. O., & Brantley, S. L. (2015). Magnesium isotope fractionation during shale weathering in the Shale Hills Critical Zone Observatory: Accumulation of light Mg isotopes in soils by clay mineral transformation. *Chemical Geology*, *397*, 37–50.

Maguire, M. E., & Cowan, J. A. (2002). Magnesium chemistry and biochemistry. *Biometals*, *15*, 203–210.

Mavromatis, V., Prokushkin, A. S., Pokrovsky, O. S., Viers, J., & Korets, M. A. (2014). Magnesium isotopes in permafrost-dominated Central Siberian larch forest watersheds. *Geochimica et Cosmochimica Acta*, *147*, 76–89.

Metson, A. (1974). Magnesium in New Zealand soils I. Some factors governing the availability of soil magnesium: A review. *New Zealand Journal of Experimental Agriculture*, *2*, 277–319.

Mile, M., & Mitkova, T. (2012). *Soil moisture retention changes in terms of mineralogical composition of clays phase. Clay Minerals in Nature - Their Characterization, Modification and Application* (pp. 101–118). Rijeka, Croatia: InTech.

Opfergelt, S., Burton, K. W., Georg, R. B., West, A. J., Guicharnaud, R. A., Sigfusson, B., ... Halliday, A. N. (2014). Magnesium retention on the soil exchange complex controlling Mg isotope variations in soils, soil solutions and vegetation in volcanic soils, Iceland. *Geochimica et Cosmochimica Acta*, *125*, 110–130.

Opfergelt, S., Georg, R. B., Delvaux, B., Cabidoche, Y. M., Burton, K. W., & Halliday, A. N. (2012). Mechanisms of magnesium isotope fractionation in volcanic soil weathering sequences, Guadeloupe. *Earth and Planetary Science Letters*, *341*, 176–185.

Pasternak, K., Kocot, J., & Horecka, A. (2010). Biochemistry of Magnesium. *Journal of Elementology*, *15*, 601–616.

Pogge von Strandmann, P. A. E., Burton, K. W., James, R. H., van Calsteren, P., Gislason, S. R., & Sigfusson, B. (2008). The influence of weathering processes on riverine magnesium isotopes in a basaltic terrain. *Earth and Planetary Science Letters*, *276*, 187–197.

Pokharel, R., Gerrits, R., Schuessler, J. A., Floor, G. H., Gorbushina, A. A., & von Blanckenburg, F. (2017). Mg isotope fractionation during uptake by a rock-inhabiting, model microcolonial fungus *Knufia petricola* at acidic and neutral pH. *Environmental Science & Technology*, *51*, 9691–9699.

Pokharel, R., Gerrits, R., Schuessler, J. A., Frings, P. J., Sobotka, R., Gorbushina, A. A., & von Blanckenburg, F. (2018). Magnesium stable isotope fractionation on a cellular level explored by cyanobacteria and black fungi with implications for higher plants. *Environmental Science & Technology*, *52*, 12216–12224.

Ryu, J. S., Vigier, N., Decarreau, A., Lee, S. W., Lee, K. S., Song, H., & Petit, S. (2016). Experimental investigation of Mg isotope fractionation during mineral dissolution and clay formation. *Chemical Geology*, *445*, 135–145.

Schmitt, A. D., Vigier, N., Lemarchand, D., Millot, R., Stille, P., & Chabaux, F. (2012). Processes controlling the stable isotope compositions of Li, B, Mg and Ca in plants, soils and waters: A review. *Comptes Rendus Geoscience*, *344*, 704–722.

Sümer, M.R. 2012. Auswirkungen verschiedener Bodennutzungssysteme auf ausgewählte physiko-chemische Bodeneigenschaften und pflanzenbauliche Parameter in Berlin-Dahlem und Dedelow. (Doctoral dissertation). Humboldt-Universität zu, Berlin, Germany.

Teng, F. Z. (2017). Magnesium isotope geochemistry. *Reviews in Mineralogy and Geochemistry*, *82*, 219–287.

Teng, F. Z., Li, W. Y., Rudnick, R. L., & Gardner, L. R. (2010). Contrasting lithium and magnesium isotope fractionation during continental weathering. *Earth and Planetary Science Letters*, *300*, 63–71.

Teng, F. Z., Wadhwa, M., & Helz, R. T. (2007). Investigation of magnesium isotope fractionation during basalt differentiation: Implications for a chondritic composition of the terrestrial mantle. *Earth and Planetary Science Letters*, *261*, 84–92.

Tipper, E. T., Galy, A., Gaillardet, J., Bickle, M. J., Elderfield, H., & Carder, E. A. (2006). The magnesium isotope budget of the modem ocean: Constraints from riverine magnesium isotope ratios. *Earth and Planetary Science Letters*, *250*, 241–253.

Tipper, E. T., Lemarchand, E., Hindshaw, R. S., Reynolds, B. C., & Bourdon, B. (2012). Seasonal sensitivity of weathering processes: Hints from magnesium isotopes in a glacial stream. *Chemical Geology*, *312*, 80–92.

Uhlig, D., Schuessler, J. A., Bouchez, J., Dixon, J. L., & von Blanckenburg, F. (2017). Quantifying nutrient uptake as driver of rock weathering in forest ecosystems by magnesium stable isotopes. *Biogeosciences*, *14*, 3111–3128.

Walter, K., Don, A., Tiemeyer, B., & Freibauer, A. (2016). Determining soil bulk density for carbon stock calculation: A systematic method comparison. *Soil Science Society of America Journal*, *80*, 579–591.

Wang, S. J., Teng, F. Z., Rudnick, R. L., & Li, S. G. (2015). The behavior of magnesium isotopes in low-grade metamorphosed mudrocks. *Geochimica et Cosmochimica Acta*, *165*, 435–448.

Wimpenny, J., Colla, C. A., Yin, Q. Z., Rustad, J. R., & Casey, W. H. (2014). Investigating the behaviour of Mg isotopes during the formation of clay minerals. *Geochimica et Cosmochimica Acta*, *128*, 178–194.

Wimpenny, J., Gislason, S. R., James, R. H., Gannoun, A., Pogge Von Strandmann, P. A. E., & Burton, K. W. (2010). The behaviour of Li and Mg isotopes during primary phase dissolution and secondary mineral formation in basalt. *Geochimica et Cosmochimica Acta*, *74*, 5259–5279.

Wimpenny, J., Yin, Q. Z., Tollstrup, D., Xie, L. W., & Sun, J. (2014). Using Mg isotope ratios to trace Cenozoic weathering changes: A case study from the Chinese Loess Plateau. *Chemical Geology*, *376*, 31–43.

Wombacher, F., Eisenhauer, A., Heuser, A., & Weyer, S. (2009). Separation of Mg, Ca and Fe from geological reference materials for stable isotope ratio analyses by MC-ICP-MS and double-spike TIMS. *Journal of Analytical Atomic Spectrometry*, *24*, 627–636.

Yadav, B. K., Akhtar, M. S., & Panwar, J. (2015). Rhizospheric plant-microbe interactions: Key factors to soil fertility and plant nutrition. In N.K. Arora (Ed.), *Plant microbes symbiosis: Applied facets* (pp. 127-145). New Delhi:Springer.

Young, E. D., & Galy, A. (2004). The isotope geochemistry and cosmochemistry of magnesium. *Geochemistry of Non-Traditional Stable Isotopes*, *55*, 197–230.

SUPPORTING INFORMATION

Additional supporting information may be found online in the Supporting Information section at the end of this article.

How to cite this article: Wang Y, Wu B, Berns AE, et al. A century of liming affects the Mg isotopic composition of the soil and crops in a long-term agricultural field at Berlin-Dahlem, Germany. *Eur J Soil Sci*. 2021;72:300–312. https://doi.org/10.1111/ejss.12951